www.arpnjournals.com

MODELING OF BRUSHLESS DOUBLY FED INDUCTION GENERATOR WITH CONVERTER CONTROL

Resmi R. and V. Vanitha
Department of Electrical and Electronics Engineering, Amrita Vishwa Vidhya Peetham, Coimbatore, India
E-Mail: resmidhun2010@gmail.com

ABSTRACT

The tremendous increase in the use of fossil fuels and rapid depletion of natural resources are lead to the alternative sources of energy which is environment friendly are renewable energy. There has been a great interest in wind energy in recent years because it is a potential source for electricity generation with minimal environmental impacts and with no cost of fuel. The usually used wind electric conversion system (WECS) based on Doubly Fed Induction Generator (DFIG) uses slip rings and brushes. Due to depreciation of the slip rings and brushes of generator maintenance is a major issue. Also it will be very difficult to access them in the case of offshore wind farm. So, Brushless Doubly-Fed Induction Generator (BDFIG) was proposed to replace the traditional DFIG. This paper deals with mathematical modeling of BDFIG based Wind Electric Generator (WEG) with converter control. Modeling is done for 5kW WEG with the help of mathematical equations governing each component using MATLAB simulink and the results are presented.

Keywords: BDFIG, WECS, WEG, voltage source, converter, ASD.

1. INTRODUCTION

Wind is the motion of air masses produced by the irregular heating of earth's surface by sun. A wind turbine which converts kinetic energy of wind into mechanical energy together with generator is commonly called as Wind Electric Generator (WEG). Brushless Doubly Fed Induction Machine is a single frame induction machine with two stator windings of different pole numbers. The two stator windings are of different frequencies, one a fixed frequency connected to the grid known as Power winding and the other known as Control winding with a variable frequency derived from a power electronic frequency converter. So the maximum power transfer can takes place through Power winding. Usage of BDFIG as a part of adjustable speed drive (ASD) system is finding to be economical because of the reduction in converter size due to reduction of the power flow through Control winding [1]. ASD has got maximum aerodynamic efficiency and hence better energy capture, mechanical stress reduction of wind turbine, acoustic noise reduction and cost effectiveness.

2. BDFIG CONFIGURATION

BDFIG has three modes of operation namely simple induction mode, cascaded induction mode and synchronous mode. In the Synchronous Mode of operation of BDFIG is similar to that of a synchronous machine in that (in the ideal case) the phase of the control winding voltage controls the torque of the machine and the magnitude of this voltage controls the reactive power flow in the machine. However, by adjusting the control winding frequency this synchronous machine like performance can be achieved at any speed. The ability to operate in the synchronous mode distinguishes the BDFIG from induction motor drives. The synchronous mode of operation occurs when the double stator windings carries the rotor current of the same frequency. A wind-turbine generator must be fully controllable so that it can operate

at a shaft speed that is dependent on wind conditions to obtain the maximum power output. Furthermore, control of reactive power is important in power generation, and therefore, the capability of the generator controller to regulate the power factor is essential. Since the BDFIG is not stable over the whole operating speed range, a controller is required to stabilize the machine while achieving satisfactory dynamic performance in controlling the speed and reactive power. The synchronous speed ω_r of the machine is given by Equation (1)

$$\omega_r = \omega_p \pm \omega_c / P_p + P_c \qquad (1)$$

where ω_p and ω_c are the electrical angular frequencies of PW and CW voltages respectively. P_p and P_c are pole pair numberes of PW and CW, respectively.
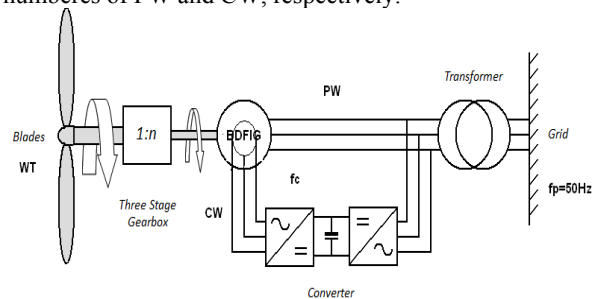
Figure-1. Schematic diagram of BDFIG based WEG.

3. MODELLING OF WECS

For the purpose of analysis of a system modeling plays a major role. So in order to study the behavior of the BDFIG a mathematical model is developed in MATLAB simulink and a back to back converter is also modeled for the purpose of controlling the variation in the wind speed for proper working of BDFIG. The major components of WEG are Wind turbine, Drive train Generator and converter. Modeling of Wind turbine, Drive train and Generator has been done [7] and presented the results.

www.arpnjournals.com

4. MODELING OF WIND TURBINE

A wind turbine is a rotating machine that converts the kinetic energy of wind into mechanical energy.

$$P_t = \rho A C_p \, v^3/2 \qquad (2)$$

where Pt is the power output from the wind turbine in watts, ρ is the air density, A is the turbine swept area and Cp is the performance coefficient or power coefficient of the wind turbine. Tip Speed Ratio (TSR) of a wind turbine, which is defined as the ratio of turbine speed at its tip to wind speed.

$$\lambda = 2 \prod NR/v \qquad (3)$$

where λ is the TSR and R is the radius of turbine swept area, N is the rotational speed of turbine in rps, v is the wind speed in m/s. C_p is the function of β and λ, where β is the pitch angle in degrees over which each turbine blade is turned for protection of WEG against high wind speed. Using these equations, development of wind turbine model can be done. Figure-2 shows the simulink model of Wind turbine [7].
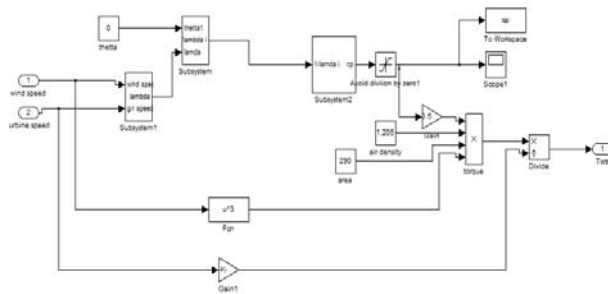
Figure-2. Model of wind turbine in simulink.

5. DRIVE TRAIN MODELING

Neglecting the stiffness and damping factor, one-mass model for the drive train is modeled using equivalent moment of inertia, equivalent wind turbine torque, generator torque and generator speed. The Simulink model for the Drive train is shown in Figure-3.
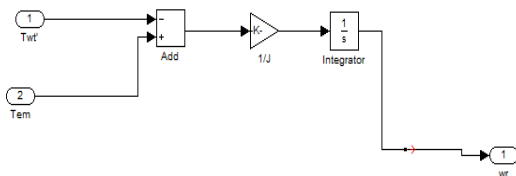
Figure-3. Simulink model of drive train.

6. BDFIG MODELING

Using Electrical Machine Analysis theory, Dynamic model of BDFIG can be obtained in dq reference frame [3], [4] and [5]. Voltage Equations for power and control windings and one rotor winding in dq frame are given by the following Equations.

$$V_{dp} = R_p \, i_{dp} + \frac{d\lambda_{dp}}{dt} - \omega_p \lambda_{pq} \qquad (4)$$

$$V_{dq} = R_p \, i_{qp} + \frac{d\lambda_{qp}}{dt} + \omega_p \lambda_{dp} \qquad (5)$$

$$V_{dc} = R_c \, i_{dc} + \frac{d\lambda_{dc}}{dt} - (\omega_p - (P_p + P_c)\omega_r)\lambda_{qc} \qquad (6)$$

$$V_{qc} = R_c \, i_{qc} + \frac{d\lambda_{qc}}{dt} + (\omega_p - (P_p + P_c)\omega_r)\lambda_{dc} \qquad (7)$$

$$V_{dr} = R_r \, i_{dr} + \frac{d\lambda_{dr}}{dt} - (\omega_p - P_p \omega_r)\lambda_{qr} \qquad (8)$$

$$V_{qr} = R_r \, i_{qr} + \frac{d\lambda_{qr}}{dt} + (\omega_p - P_p \omega_r)\lambda_{dr} \qquad (9)$$

The active and reactive power through PW and CW are given by the Equations,

$$P_p = \frac{3}{2}(V_{dp} \, i_{dp} + V_{qp} \, i_{qp}) \qquad (10)$$

$$Q_p = \frac{3}{2}(V_{qp} \, i_{dp} - V_{dp} \, i_{qp}) \qquad (11)$$

$$P_c = \frac{3}{2}(V_{dc} \, i_{dc} + V_{qc} \, i_{qc}) \qquad (12)$$

$$Q_c = \frac{3}{2}(V_{qc} \, i_{dc} - V_{dc} \, i_{qc}) \qquad (13)$$

where V_{dp} & V_{qp} are Power winding voltages, V_{dc} & V_{qc} are Control winding voltages, V_{dr} & V_{qr} are rotor voltages, i_{dp} & i_{qp} are power winding currents, i_{dc} & i_{qc} are control winding currents, i_{dr} & i_{qr} are rotor currents, L_p –self inductance of power winding, L_c – self inductance of control winding, L_r –self inductance of rotor, M_p- mutual inductance between power winding and rotor, M_c- mutual inductance between control winding and rotor, R_p- resistance of power winding, R_c- resistance of control winding, R_r-resistance of rotor.
Using all above equations, BDFIG model is developed. Figure-4 shows the complete model of BDFIG based WEG in MATLAB Simulink [7].
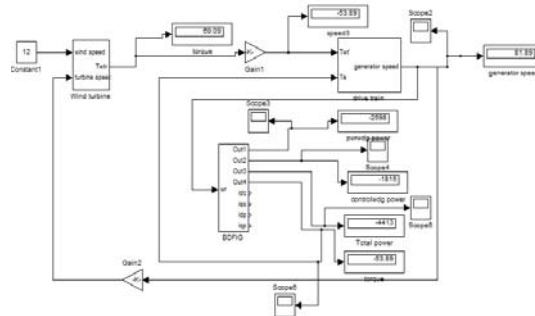
Figure-4. Complete model of BDFIG based WEG.

www.arpnjournals.com

7. MODELLING OF BACK TO BACK CONVERTER

Now a days in wind turbine applications the back-to-back voltage source converter (VSC) is mainly used [6]. A block diagram of back to back VSC is shown in Figure-5.
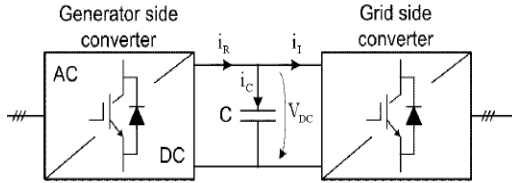
Figure-5. Structure of the back-to-back voltage source converter.

This topology comprises a double conversion from AC to DC and then from DC to AC. Both converters can operate in rectifier or inverter mode and therefore a bi-directional power flow can be achieved. When the machine acting as a generator, machine side converter act as a rectifier and grid side converter act as an inverter and vice versa for the motoring mode. Here only the generating mode is considered. So, modeling is done for a three phase diode bridge rectifier and an inverter with control [2]. When a Voltage Source Converter is used in conjunction with a star connected machine, (squirrel-cage or wound rotor) is shown in Figure-6.
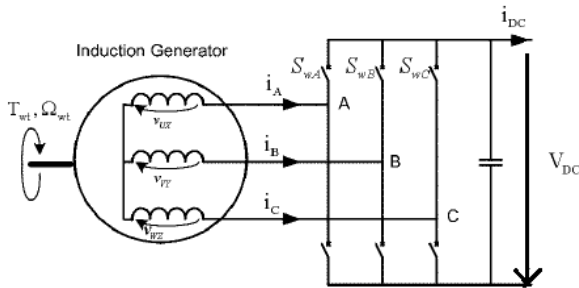
Figure-6. Star connected induction machine with a VSC.
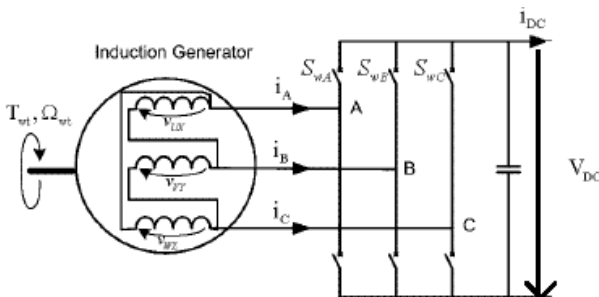
Figure-7. Delta connected induction machine with a VSC.

The applied voltages at the machine terminals as a function of the DC-link voltage and the switching functions are given as:

$$\begin{bmatrix} v_{UX} \\ v_{VY} \\ v_{WZ} \end{bmatrix} = \frac{1}{3} V_{DC} \begin{bmatrix} 2 & -1 & -1 \\ -1 & 2 & -1 \\ -1 & -1 & 2 \end{bmatrix} \begin{bmatrix} S_{wA} \\ S_{wB} \\ S_{wC} \end{bmatrix} \tag{14}$$

When a Voltage Source Converter is used in conjunction with a delta connected machine shown in Figure.7.The applied voltages at the machine terminals as a function of the DC-link voltage and the switching functions are given here:

$$\begin{bmatrix} v_{UX} \\ v_{VY} \\ v_{WZ} \end{bmatrix} = V_{DC} \begin{bmatrix} 1 & -1 & 0 \\ 0 & 1 & -1 \\ -1 & 0 & 1 \end{bmatrix} \begin{bmatrix} S_{wA} \\ S_{wB} \\ S_{wC} \end{bmatrix} \tag{15}$$

The DC-link current can be expressed as a function of the input currents and the switching functions are given by:

$$i_{DC} = \begin{bmatrix} S_{wA} & S_{wB} & S_{wC} \end{bmatrix} \begin{bmatrix} i_A \\ i_B \\ i_C \end{bmatrix} \tag{16}$$

a) Modeling of three phase diode Bridge rectifier using switching functions

Three phase diode bridge rectifier circuit configuration is shown in Figure.6.The diode bridge behaviour can be described in terms of suited switching functions called $g(i)$ the Heaviside step function:

$$V_{1N} = g(i_1)v_d \;,\; V_{2N} = g(i_2)v_d \;,\; V_{3N} = g(i_3)v_d \tag{17}$$

When the current in each phase is greater than or equal to zero, diodes in the corresponding phase becomes turn on otherwise becomes off. For phase A, D1 &D2 is ON. For phase B, D3 & D4 is ON. For phase C, D5 & D6 is ON which is shown in Figure-8.
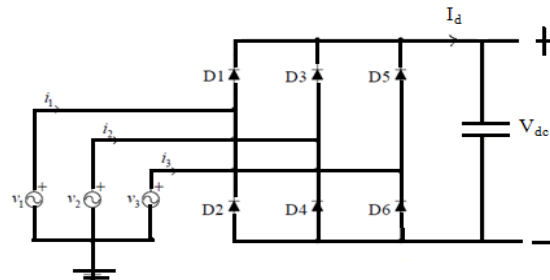
Figure-8. Rectifier circuit configuration.

Voltages V_{1N}, V_{2N}, V_{3N} can be expressed as

$$V_{1N} = g(i_1)v_d \;,\; V_{2N} = g(i_2)v_d \;,\; V_{3N} = g(i_3)v_d$$

while the output bridge current

$$i_d = g(i_1)* i_1 + g(i_2)* i_2 + g(i_3)*i_3 \tag{18}$$
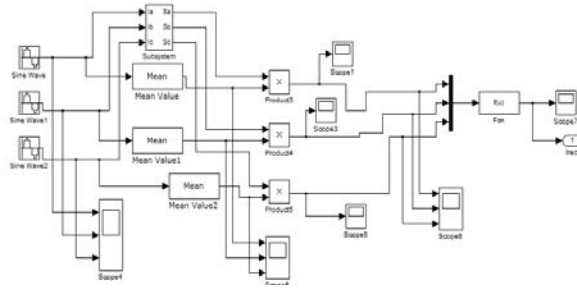
Figure-9. Simulnk model of three phase diode bridge rectifier.

b) Modeling of Inverter Circuit with control

Hysteresis Current Control (HCC) is method is used to switch the inverter. HCC is the easiest control method to implement; it was developed by Brod and Novotny in 1985. The current controller decides the switching patterns of the devices in the inverter. The dc voltage across the capacitor is sensed and is compared with the reference and the error is processed in the PI controller to generate a current reference I_d^*.Similarly, grid voltage is sensed and is compared with the reference and the error is processed in the PI controller to generate another current reference I_q^*.This I_d^* and I_q^* is converted to I_{abc}^* using dq-abc transformation and it is compared with measured grid current I_{abc} in Hysteresis Controller.
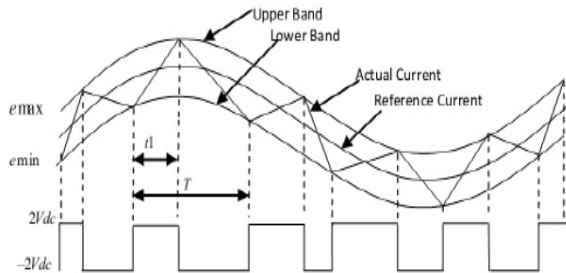
Figure-10. Hysteresis current control.

I_{abc}^* and I_{abc} are the inputs to the hysteresis controller. An error signal is used to control the switches in a voltage source inverter. This error is the difference between the desired current and the current being injected by the inverter. If the error exceeds the upper limit of the hysteresis band, the upper switch of the inverter arm is turned off and the lower switch is turned on. As a result, the current starts decaying. If the error crosses the lower limit of the hysteresis band, the lower switch of the inverter arm is turned off and the upper switch is turned on. As a result, the current gets back into the hysteresis band. The range of the error signal e_{max} - e_{min} directly controls the amount of ripple in the output current from the VSI. Thus both real and reactive power can be controlled. Block diagram of inverter control used is shown in Figure-10
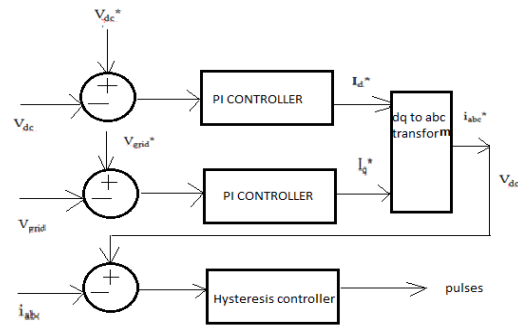
Figure-11. Block diagram of inverter control

c) DC Link Circuit

Typically, the DC-link circuit is represented as an ideal capacitor as shown in Figure-8. The DC-link voltage V_{DC}, which is the voltage at the capacitor terminals, is given by:

$$v_{DC} = \frac{1}{C} \int i_C dt = \frac{1}{C} \int (i_R - i_I) \, dt$$

(17)

where I_R is the rectifier output current in Ampere , I_I is the inverter input current in Ampere and C is the capacitance value in Farad [5].
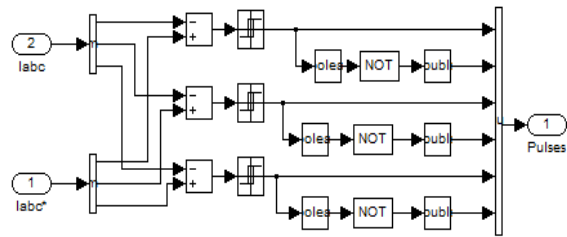
Figure-12. Simulink model of hysteresis current controller.
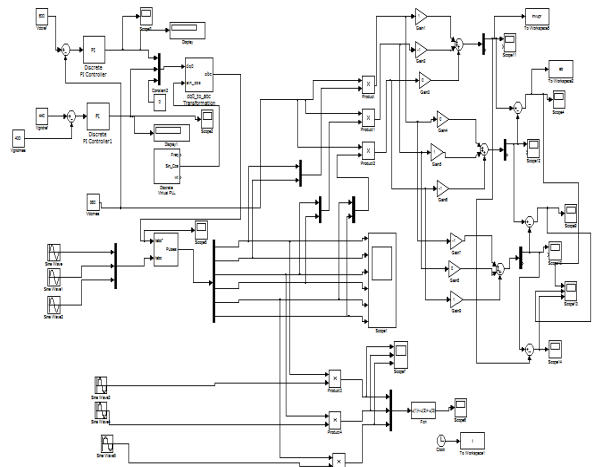
Figure-13. Simulink model of Inverter with control.

www.arpnjournals.com

8. SIMULATION RESULTS

a) Simulation results of BDFIG based WEG

5kW Brushless Doubly Fed Induction Generator is modeled to get the following data.

Table-1. Variation in BDFIG power for different wind speeds.

Wind speed (m/s)	Real power (kW) in PW	Real power (kW) in CW	Total real power (kW)
2	0.02305	0.52845	0.5515
4	0.1634	1.1446	1.308
6	0.5516	1.3094	1.861
8	0.805	1.748	2.553
10	1.85	1.549	3.399
12	2.605	1.807	4.412
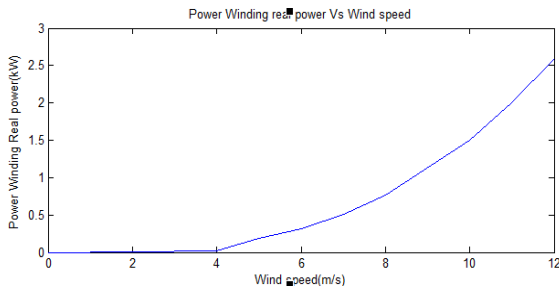
Figure-14. Power Winding real power vs wind speed.

Simulation of BDFIG is run for different wind speeds and Figure-14, 15 and 16 shows the graphical results. The corresponding readings are tabulated in Table-1.
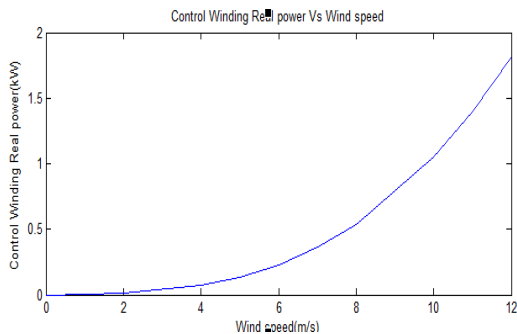
Figure-15. Control winding real power vs wind speed.
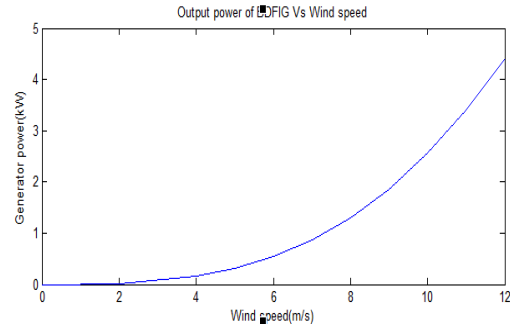
Figure-16. Total output power of BDFIG Vs wind speed.

Figure-17 shows the variation in BDFIG power from 1.308kW to 4.413kW when wind speed is changed from 8m/s to 12m/s, ie cut in speed to rated speed.
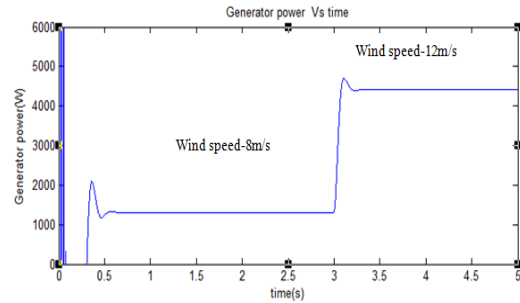
Figure-17. BDFIG power for change in wind speed.

b) Simulation results of Back to Back Converter
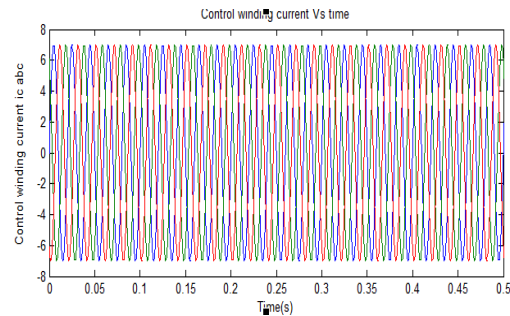
Figure-18. Input current waveform of 3 phase rectifier.
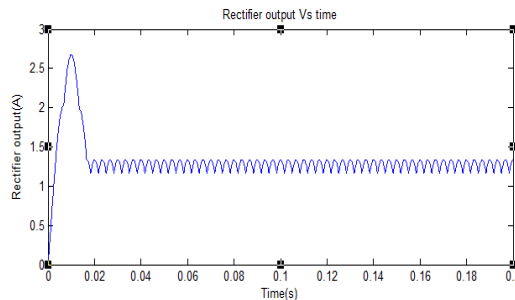
Figure-19. Output current waveform of 3 phase rectifier.
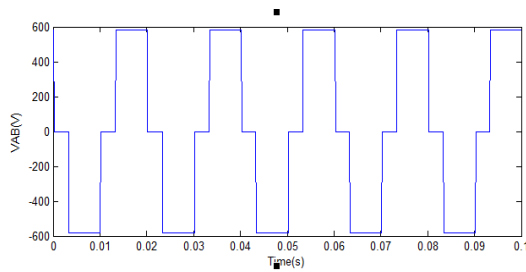
Figure-20. Output voltage waveforms in a phase of grid side inverter.
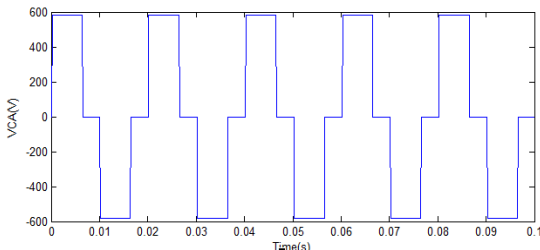
Figure-21. Output voltage waveforms in B phase of grid side inverter.
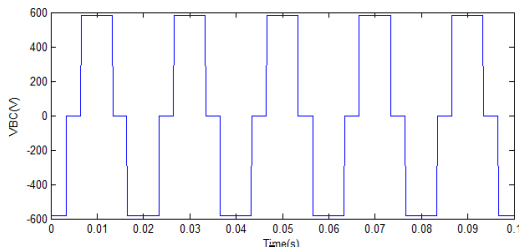
Figure-22. Output voltage waveforms in C phase of grid side inverter.

Simulation results from the rectifier circuit are given in Figure-18 and Figure-19. The rectified pulse obtained can be connected to the inverter side through the designed DC link capacitor. From the designed inverter the three phase pulses obtained properly are presented in Figure-20, 21 and 22.

9. CONCLUSIONS

In this paper study about the BDFIG based WECS has been carried out by constructing the simulink model of the same in MATLAB. Main application of this wind electric generator will be in offshore wind farms because of the reliability in maintenance due to absence of brushes. The introduction of two stator windings in to the machine made the power electronics side of the system economically better. Simulation results of BDFIG works as WEG shows that a wide range of speed variation and effective power generation is possible. The control part of the system consists of a three phase diode rectifier and a three phase inverter. Modeling of that has been done using hysteresis current control, implemented in MATLAB platform and obtained relevant results. By using this BDFIG with variable speed wind turbine to track maximum power from wind turbine for the given wind speed is possible. This work can be extended with pitch control to track the maximum power point in the turbine power curve.

REFERENCES

[1] R. A. McMahon, P. C. Roberts, X. Wang and P. J. Tavner. 2006. "Performance of BDFM as generator and motor," in IET Proceedings, Electric Power Applications, Vol. 153, no. 2, pp. 289 – 299.

[2] A. Di Gerlando, G. Foglia, M. Iacchetti and R. Perini. 2010. "Analytical Model and Implementation by Equations of Three-Phase Diode Bridge Rectifiers Operation", XIX International Conference on Electrical Machines - ICEM pp: 978 – 982.

[3] Shiyi Shao, Ehsan Abdi, Farhad Barati and Richard McMahon. 2009. "Stator-Flux-Oriented Vector Control for Brushless Doubly Fed Induction Generator", IEEE Transactions on Industrial Electronics, Vol. 56, No. 10, October.

[4] Kostyantyn Protsenko and Dewei Xu. 2008. "Modelling and Control of Brushless Doubly-Fed Induction Generators in Wind Energy Applications",IEEE Transactions on power electronics, Vol. 23, No. 3, May.

[5] Chun Liu1,David Xu and Xing Zhang. 2011. "Dynamic Performance of Brushless Doubly-fed Induction Generator during Symmetrical Grid Fault", 8th International Conference on Power Electronics, June 3.

[6] Ladoux P., Postiglione G., Foch H. and Nuns J. 2005. "A Comparative Study of AC/DC Converters for High-Power DC Arc Furnace," IEEE Trans. Indus. Electron., Vol. 52, No. 3, pp. 747-757, June.

[7] Anjana Suresh, Resmi R. and Dr. Vanitha V. 2015. "Mathematical model of Brushless Doubly Fed Induction Generator based Wind Electric Generator", Power Electronics and Renewable Energy Systems, Lecture Notes in Electrical Engineering, Vol. 326, pp. 1477-1487.